Trypanosome REH1 is an RNA helicase involved with the 3′–5′ polarity of multiple gRNA-guided uridine insertion/deletion RNA editing

Feng Li[a,1], Jeremy Herrera[a], Sharleen Zhou[b], Dmitri A. Maslov[c], and Larry Simpson[a,1]

[a]Department of Microbiology, Immunology and Molecular Genetics, David Geffen School of Medicine at University of California, Los Angeles, CA 90095; [b]Howard Hughes Medical Institute Mass Spectrometry Laboratory, University of California, Berkeley, CA 94720; and [c]Department of Biology, University of California, Riverside, CA 92521

Edited by Joan A. Steitz, Howard Hughes Medical Institute, New Haven, CT, and approved January 4, 2011 (received for review September 22, 2010)

Uridine insertion/deletion RNA editing in kinetoplastid mitochondria corrects encoded frameshifts in mRNAs. The genetic information for editing resides in small guide RNAs (gRNAs), which form anchor duplexes just downstream of an editing site and mediate editing within a single editing "block." Many mRNAs require multiple gRNAs; the observed overall 3′ to 5′ polarity of editing is determined by the formation of upstream mRNA anchors by downstream editing. Hel61, a mitochondrial DEAD-box protein, was previously shown to be involved in RNA editing, but the functional role was not clear. Here we report that down-regulation of Hel61 [renamed REH1 (RNA editing helicase 1)] expression in *Trypanosoma brucei* selectively affects editing mediated by two or more overlapping gRNAs but has no effect on editing within a single block. Down-regulation produces an increased abundance of the gRNA/edited mRNA duplex for the first editing block of the A6 mRNA. Recombinant REH1 has an ATP-dependent double strand RNA unwinding activity in vitro with a model gRNA-mRNA duplex. These data indicate that REH1 is involved in gRNA displacement either directly by unwinding the gRNA/edited mRNA duplex or indirectly, to allow the 5′ adjacent upstream gRNA to form an anchor duplex with the edited mRNA to initiate another block of editing. Purified tagged REH1 is associated with the RNA editing core complex by RNA linkers and a colocalization of REH1, REL1, and two kinetoplast ribosomal proteins with the kinetoplast DNA was observed by immunofluorescence, suggesting that editing, transcription, and translation may be functionally linked.

Leishmania | RNAi | tandem affinity purification | streptavidin binding and protein A purification

Uridine insertion/deletion RNA editing (1, 2) in the mitochondria of kinetoplastid protists is an essential process that results in the correction of encoded frameshifts thereby rendering the mRNAs translatable. The reaction involves the interaction of "preedited" mRNAs transcribed from maxicircle kinetoplast DNA with small gRNAs that act as templates for the precise insertion and deletion of uridylyl residues at multiple sites (3). The editing reaction is mediated by a holoenzyme or "editosome" (4). The core component of the editosome is the RECC (RNA editing core complex) (5) that contains approximately 15–20 polypeptides (2, 6–9). Eight RECC proteins have been so far functionally characterized. The remaining proteins contain a variety of motifs including zinc fingers, single-strand binding (SSB), and OB folds, and the roles of these proteins in the editing reaction are not known, although several are required for structural stability of the RECC. Low-resolution cryoEM 3D structures for RECC particles from *Trypanosoma brucei* and *Leishmania tarentolae* have been published (7, 10), but these do not have sufficient resolution to shed light on the precise mechanisms involved in the editing reactions.

Several multiprotein complexes have been described that interact with the RECC via RNA in substoichiometric amounts. These include the MRP1/2 complex (11, 12) and the guide RNA binding complex (GRBC)/mitochondrial RNA binding (MRB1) complex (13–16). Heterogeneous-sized high molecular weight complexes (L* or RECC*) consisting of the RECC together with several RNA-linked complexes have been visualized by electrophoresis in blue native gels (4). These break down with RNase treatment, giving rise to the 1-MDa RECC, and we have suggested that they may represent the holoenzyme (4).

The initial editing event occurs when a gRNA forms an RNA duplex with a complementary mRNA sequence just downstream of the editing site (3). A single gRNA encodes the information for several adjacent editing sites; this constitutes an "editing block." RNA editing has a 3′ to 5′ polarity within a single block (3) due to the fact that the gRNA first forms a duplex anchor just downstream of an editing site. Insertion and deletion of u residues occurs at the first gRNA/mRNA mismatch. This extends the mRNA-gRNA duplex in a 5′ direction and editing is then reinitiated at the next upstream editing site. However, "misedited" sequences occur that are due in some cases to the hybridization of the incorrect gRNA and in other cases apparently to stochastic errors in the editing mechanism. Alternative editing has been identified in several mRNAs that contain multiple gRNA-mediated editing domains (17). This mechanism would greatly increase the repertoire of proteins, but confirmation of this phenomenon and its generality remain to be examined.

The editing of most mRNAs is mediated by multiple overlapping gRNAs. Editing utilizing the adjacent upstream gRNA cannot proceed until the first block is completely edited because the gRNA can only form an anchor duplex with edited sequence to initiate the second editing block. This is responsible for the observed overall 3′ to 5′ polarity (18), but the mechanism of displacement of adjacent gRNAs is unknown. An RNA helicase has been suggested to be involved in this process by displacing the initial gRNA, thereby allowing the adjacent upstream gRNA to form an anchor duplex with the edited sequence (19). Two trypanosome mitochondrial DExD/H-box proteins have been identified (14, 16, 20, 21) and shown to be involved in RNA editing. RNA editing helicase 2 or REH2 is a component of GRBC or MRB1 complexes and is involved in gRNA biogenesis (13, 14, 16). Hel61, another DEAD-box protein, was shown to be involved in RNA editing by a gene disruption experiment in *T. brucei*, which produced a slow growth phenotype and affected editing efficiency, and ectopic reexpression of Hel61 rescued a partially restored editing phenotype (21). However, gene disruption had no effect on either an experimentally observed mito-

Author contributions: F.L., D.A.M., and L.S. designed research; F.L., J.H., S.Z., and D.A.M. performed research; F.L. and L.S. analyzed data; and F.L., D.A.M., and L.S. wrote the paper.

The authors declare no conflict of interest.

This article is a PNAS Direct Submission.

[1]To whom correspondence may be addressed. E-mail: fengli@ucla.edu or larrys3255@gmail.com.

This article contains supporting information online at www.pnas.org/lookup/suppl/doi:10.1073/pnas.1014152108/-/DCSupplemental.

chondrial RNA unwinding activity (20) or on full cycle in vitro editing reactions (21). Furthermore, the observed RNA unwinding activity did not cosediment with Hel61 (21). The functional role of Hel61 and the mechanism of gRNA displacement were not clear.

In this paper we present evidence that Hel61 is involved in the displacement of gRNAs to allow the 5′ adjacent gRNA to form an anchor duplex with the edited sequence. We also show that recombinant REH1 has ATP-dependent duplex RNA unwinding activity. We have therefore relabeled Hel61 with the functional name, REH1 (RNA editing helicase 1).

Results

Effect of Down-Regulation of REH1 Expression in *T. brucei* on Relative Abundance of mRNAs Edited in Block 1 Versus Those Edited in Two or More Blocks. Down-regulation of expression of REH1 by conditional RNAi in *T. brucei* procyclic cells produced a slow growth phenotype (Fig. 1*A*). An 80% decrease in the abundance of REH1 mRNA by day 3 was demonstrated by RT-PCR and real-time RT-PCR (Fig. 1 *B* and *D*) and REH1 protein was not detectable by Western blot analysis (Fig. 1*B*). Repression of REH1 expression showed no effect on the stability or length of the gRNA 3′ oligo U tails (Fig. 1*C*), as was reported for the trypanosome REH2 mitochondrial RNA helicase (14, 16)

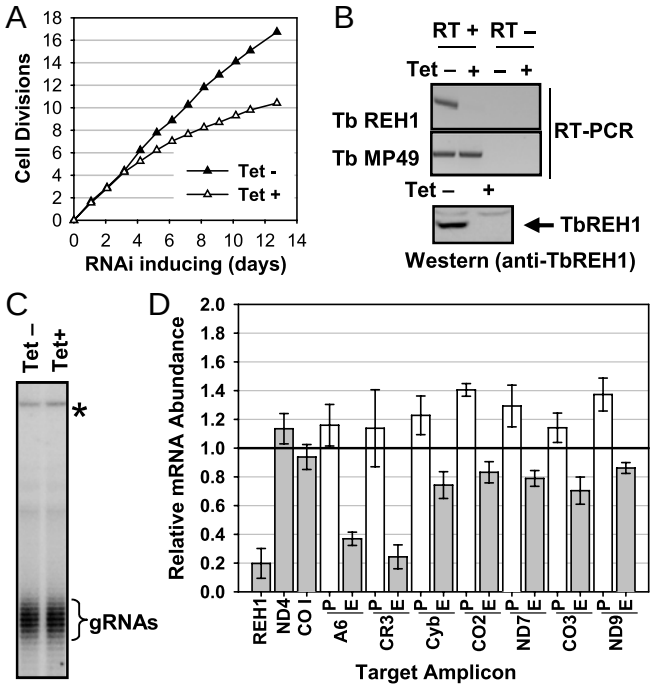

Fig. 1. Effect of RNAi down-regulation of REH1 expression on editing in procyclic *T. brucei* cells. (*A*) Growth curve of *T. brucei* strain 2913 procyclic cells after induction of RNAi by addition of tetracycline. (*B*, *Upper*) RT-PCR of RNA from Tet+ and Tet– cells using primers for REH1. The RT– lanes are a control for contamination with DNA. RT-PCR of MP49 RNA was also performed as a loading control. (*Lower*) Western blot analysis of expression of REH1 in Tet+ and Tet– cells with anti-REH1 antibody. (*C*) Lack of effect of REH1 down-regulation on gRNAs. Total gRNA from control cells and cells 3 d after tetracycline addition was 5′ end labeled with [α-^{32}P]GTP using guanylyl transferase. The gRNAs appear as ladders due to the heterogeneous 3′-oligo(U) tails. The top band marked with "*" is a cytosolic RNA that is also labeled and was used as a loading control. (*D*) Real-time RT-PCR analysis of relative abundance of preedited (clear bars) and mature edited (gray bars) mRNAs for several maxicircle genes from *T. brucei* procyclic cells after 3-d down-regulation of REH1 expression. The ND4 and COI mRNAs, which are not edited, are used as controls. The ordinate represents the relative abundance of each mRNA compared to that of the same RNA from Tet– cells (set at 1.0). The genes are indicated below each set of bars. Error bars indicate one standard deviation.

Real-time RT-PCR was also used to quantitate the effect of REH1 down-regulation on the relative abundance of several preedited and mature edited mRNAs (Fig. 1*D* and Table S1). The abundances of edited CR3 and A6 mRNAs were significantly reduced with down-regulation of REH1, but the effects on edited mRNAs for Cyb, ND7, CO3, and ND9 were small and probably not significant because a similar decrease was observed for the CO2 edited mRNA, which is mediated by a single *in cis* gRNA and does not require an overlapping gRNA. Interestingly, the abundances of preedited mRNAs for CO2 and ND9 were increased 30–40%, raising the possibility that REH1 has an effect on RNA turnover of some mRNAs. Two never-edited RNAs, ND4 and COI, were examined as controls: Neither showed a significant change in abundance. The changes in the abundances of the A6, CR3, Cyb, ND7, and CO3 preedited mRNAs were not statistically significant.

One possible mechanism for the inhibition of editing by REH1 down-regulation is that REH1 is involved with displacement of the gRNA from the edited mRNA/gRNA duplex. To test this hypothesis, we quantitatively compared the effect of down-regulation of REH1 expression on the relative abundance of mRNAs edited in block 1 versus those edited in block 1 and the adjacent upstream blocks. The experimental protocol is diagrammed in Fig. 2*A* (also see Table S1). The only *T. brucei* genes for which putative gRNAs are known for the 3′-most editing blocks are A6 and Cyb (Figs. S1 and S2) (22, 23). Real-time RT-PCR was used to measure the relative abundances of *T. brucei* partially edited A6 and Cyb mRNAs after 3 d of REH1 RNAi compared to these mRNAs in cells without induction of RNAi. Down-regulation caused an increase of around 20% in the A6 mRNAs completely edited in block 1 (and also the preedited A6 mRNAs). On the other hand, there was a decrease of around 20% in A6 mRNAs edited in both blocks 1 and 2 and a decrease of around 40% in A6 mRNAs edited in blocks 1, 2, and 3 (Fig. 2*B*). It was noted that the primers for edited A6 mRNA in Fig. 1*D* are located near the 5′ end of A6 gene. Repression of REH1 expression caused an increase of around 20–30% in both the preedited Cyb mRNA and Cyb mRNA completely edited in block 1 and caused a decrease of around 20% in the mature Cyb mRNA edited in both blocks 1 and 2 (there are only two editing blocks in Cyb) (Fig. 2*C*). Thus, down-regulation of REH1 expression in *T. brucei* selectively affects editing that is mediated by two or more overlapping gRNAs but does not affect editing occurring within a single gRNA-mediated editing block. This result is consistent with a role in gRNA displacement.

Effect of Down-Regulation of REH1 Expression on Relative Abundance of Block 1 Edited mRNA/gRNA Duplex. Another prediction is that REH1 down-regulation would produce an increased abundance of a block 1-fully edited mRNA/gRNA duplex by inhibiting the progression of editing from block 1 to block 2. The relative abundance of this duplex was assayed by an RNase protection experiment in which poisoned primer extension using a primer complementary to fully edited block 1 mRNA was used to measure the abundance of the RNase-protected duplex RNA. The experimental protocol is diagrammed in Fig. 3*A*. As shown in Fig. 3*B*, lanes 2 and 4, there is a significant increase in the relative abundance of the RNase-protected block 1 duplex after down-regulation of REH1 expression. Although the primer covers two U-deletion and two U-insertion sites, there is no significant decrease in the no RNase control band in lanes 1 and 3, indicating that down-regulation of REH1 has no effect on intra-block editing. We conclude that REH1 is required for releasing gRNA from A6 mRNA that is completely edited in block 1.

Recombinant Streptavidin-Binding Motif (SBP)-tagged REH1 has RNA-dependent ATPase and Double Strand RNA Unwinding Activities. REH1 has conserved motifs found in DEAD-box proteins

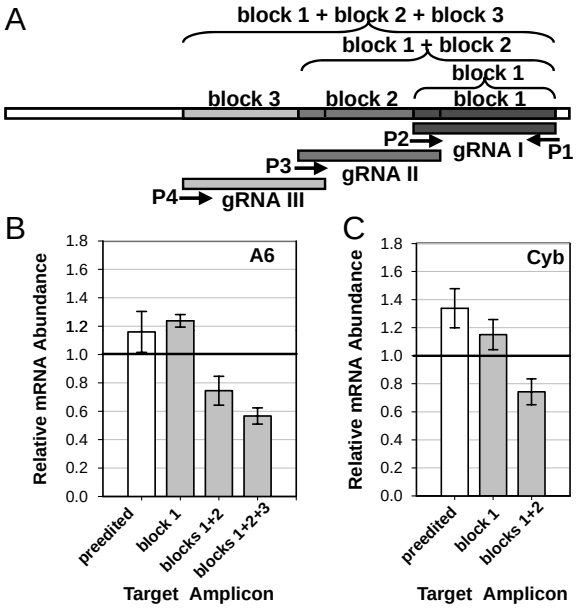

Fig. 2. Effect of repression of REH1 *T. brucei* on relative abundances of A6 and Cyb mRNAs edited in block 1 versus mRNAs edited in both blocks 1 and 2 and 3. (*A*) Diagram of real-time RT-PCR analysis. Primer sets are indicated with arrows. See Table S1 for sequences. (*B*) Relative abundance of A6 mRNAs in *T. brucei* procyclic cells induced for down-regulation of expression of REH1 by RNAi. The abundance of these mRNAs from untreated cells is set at 1.0. Clear bar, preedited mRNA; gray bars, partially edited mRNAs. (*C*) Relative abundance of Cyb mRNAs in *T. brucei* procyclic cells induced for down-regulation of expression of REH1 by RNAi. See *B* for details. The difference between the effect of RNAi on the abundance of the A6 edited mRNA and the results in this experiment are due to the use of an upstream primer near the 5′ end of the mRNA in Fig. 1*D* instead of the primer used in this assay, which is close to the 3′ end.

(Fig. 4*A* and Fig. S3), but there is no evidence in the literature for REH1 having RNA helicase activity. To address this question, we expressed tagged *Leishmania major* (Lm) REH1 (Fig. 4*B*) in Sf9 cells and analyzed the activity. A modified tandem affinity purification (TAP) tag (24), the streptavidin binding and protein A purification (SAP) tag (Fig. 4*B*), was used in which the calmodulin binding peptide motif was substituted with a high affinity streptavidin binding peptide (SBP) motif. The rREH1 was purified to homogeneity by IgG-Sepharose binding, MonoS ion-exchange chromatography, and streptavidin affinity chromatography (Fig. 4*C*, lane 1). The expressed band was confirmed to be SBP-tagged REH1 by Western analysis using anti-REH1 or HRP-conjugated streptavidin (SA-HRP) (Fig. 4*C*, lanes 2, 3). His6x-tagged REH1 was also expressed in *Escherichia coli* and purified to homogeneity for antibody generation.

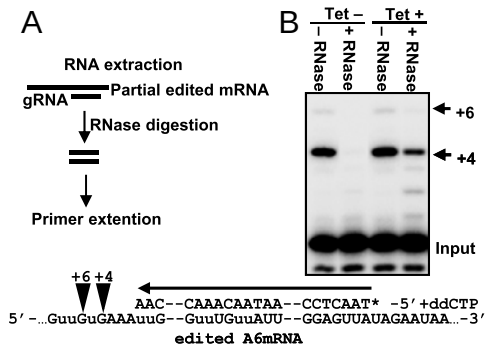

Fig. 3. Relative abundance of the *T. brucei* gRNA I/edited A6 block 1 mRNA duplex after RNAi down-regulation of REH1 expression. (*A*) Diagram of assay. The abundance is assayed by poisoned primer extension of RNase-protected A6 mRNA. (*B*) Poisoned primer extension assay of RNase-resistant A6 block 1 duplex RNA with and without down-regulation of REH1 expression. Note the presence of a +4 labeled band only in the +Tet, +RNase lane. (*Lower*) Diagram of the extension reaction.

The purified SBP-tagged recombinant REH1 protein showed a robust poly U–stimulated ATPase activity. This activity was destroyed by RNase treatment (Fig. 4*D*). As a control for ATPase contamination from the Sf9 cells, SAP-tagged RET2 RECC protein was expressed and purified using the same procedure. The tagged RET2 did not show ATPase activity (Fig. 4*D*). The REH1 ATPase activity requires ATP or dATP (Fig. S4 *D* and *E*). The optimal pH is around 8.3, the K_m for the reaction is 620 μM ATP, and the K_{cat} is 82.3 min^{-1} (Fig. S4 *A*–*C*).

Recombinant REH1 showed an ATP-dependent double strand RNA unwinding activity using a partially edited model gRNA/edited mRNA duplex (Fig. 4*E* and Table S2). The reaction required ATP and showed a protein dose response (Fig. 4 *E* and *F*). We also tested the unwinding of shorter RNA duplexes with 5′ or 3′ overhangs or no overhang (Fig. 4 *F*–*H*). The latter were unwound more efficiently probably due to their lower stability. It has been shown that helicase activity in vitro shows an inverse relationship between duplex stability and unwinding (25). As a control, a mutation of K143A in motif I, which is the conserved ATP binding domain of REH1, was introduced and the mutant protein lost ATPase and unwinding activities (Fig. S5). These data indicate that REH1 is an ATP-dependent RNA helicase. The REH1 helicase apparently differs from most other DEAD-box RNA helicases that exhibit very poor in vitro unwinding activity and require a 5′ or 3′ single-stranded RNA region for unwinding activity (25).

REH1, REL1, and the Kinetoplast Ribosome Proteins, L3 and S17, Show Concentration in the Kinetoplast Region of the Mitochondrion. Immunolocalization of SAP-tagged REH1 within the single mitochondrion of transfected *L. tarentolae* cells was performed using an antibody against the C-terminal FLAG epitope (Fig. 5*A*). This antibody does not have cross-reactivity with any endogenous protein (Fig. S6*D*). The cells were stained with MitoTracker Red to visualize the single mitochondrion and costained with DAPI to detect the nuclear and kinetoplast DNA, and then treated with anti-FLAG antibody and secondary anti-IgG antibody conjugated with Alexa Fluor 488 to visualize SAP-tagged REH1. The REH1 protein colocalized with the MitoTracker mitochondrial image. Interestingly, in addition to a dispersed localization throughout the tubular mitochondrion there is an apparent concentration of REH1 protein in the kinetoplast DNA-containing region. Lower resolution images of entire fields that show that the selected fields in Fig. 5*A* are representative are shown in Fig. S6*A*. As a control, cells were analyzed for the localization of glutamate dehydrogenase, a soluble mitochondrial protein not involved in RNA editing (Fig. S6*C*). These cells showed a somewhat punctate distribution of immunofluorescence throughout the mitochondrion without the level of concentration in the kinetoplast region observed in the REH1 immunofluorescence, indicating that the observed kinetoplast concentration of REH1 is probably not artifactual (Fig. S6).

The localizations of TAP-tagged REL1 RNA ligase, a RECC core component, and two TAP-tagged kinetoplast ribosome proteins (Fig. S6*E*), S17 and L3, were also analyzed by indirect immunofluorescence. REL1 and the two ribosome proteins showed a similar kinetoplast concentration as the SAP-tagged REH1 (Fig. 5 *B*–*D* and Fig. S6*B*).

REH1 Is Associated with the RECC by RNA Linkers. To investigate possible interactions between REH1 and the RECC, SAP-tagged Lm REH1 with a mitochondrial target signal was expressed in *L. tarentolae*. The tagged REH1 was found only in the whole cell

BIOCHEMISTRY

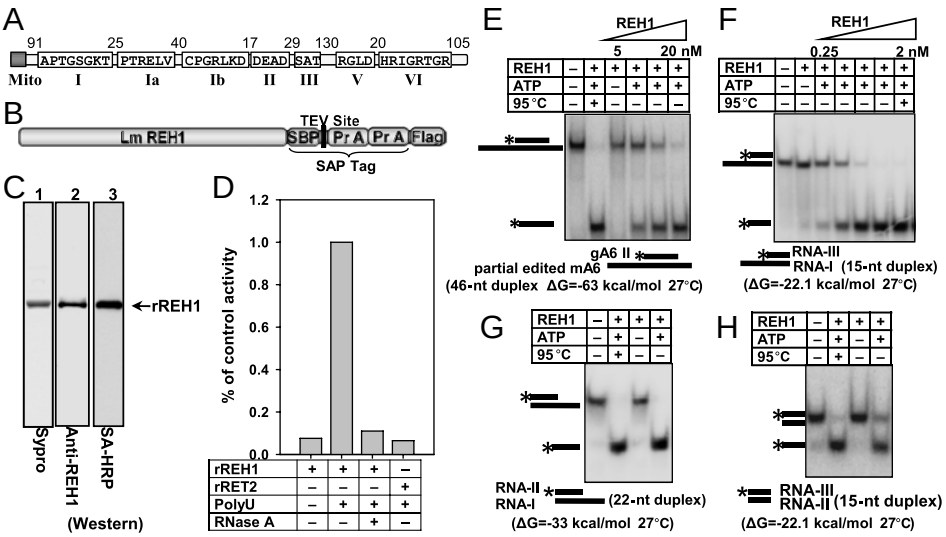

Fig. 4. Purification, RNA-dependent ATPase activity, and ATP-dependent double strand RNA unwinding activity of recombinant SBP-tagged REH1. (*A*) Diagram showing the conserved motifs of REH1. Open boxes represent the conserved helicase motifs with the indicated the amino acid sequences. The number of amino acids separating the motifs is shown. (*B*) Diagram of the SAP-tagged Lm REH1. SBP, streptavidin-binding peptide; PrA, protein (A). (*C*) Purification of SBP-tagged rREH1 expressed in sf9 insect cells using the Baculovirus expression system (Invitrogen). SDS gels stained with Sypro. Blots probed with SA-HRP or anti-REH1 antibody. (*D*) RNA-dependent ATPase activity of purified SBP-tagged REH1. The ATPase reactions were performed without added RNA, with added poly U, or with added poly U plus 0.05 mg/mL RNase. (*E*) Model gRNA/mRNA substrate with a 46-bp duplex and a 49-nt 3′ overhang. The ^{32}P-labeled end is indicated by * in the diagram. The unwinding reaction required ATP and showed a dose response with the amount of protein. (*F*) Model gRNA/mRNA substrate with a 15-bp duplex and a 24-nt 3′ overhang; 5 nM rREH1. (*G*) 22-bp duplex with 15-nt 5′ overhang; 5 nM rREH1. (*H*) 15-bp blunt end duplex; 5 nM rREH1.

and mitochondrial fractions and not in the cytosol fraction (Fig. S7*A*). Cell lysate was allowed to bind to IgG-Sepharose, and the bound material was released by digestion with tobacco etch virus (TEV) protease. Half of the eluted material was treated with RNase A prior to fractionation on a glycerol gradient. Gradient fractions were subjected to blue native gel electrophoresis and the blots probed with anti-REH1 antibody (Fig. 6*A*, *Upper*).

Autoadenylation of REL1/2 with [α-^{32}P]ATP (26) was also used to detect REL1 as a marker for the RECC (Fig. 6*A*, *Lower*). The gradient fractions were run in SDS gels that were probed with anti-REH1 antibody and with anti-MRP1/2 antibody (Fig. 6*B*). MRP1/2 are proteins that are known to associate with the RECC via RNA linkers (11).

The tagged REH1 sedimented as free oligomeric protein in the 5–10S region. A portion of the REH1 sedimented in the 20–25S region migrating in the blue native gel at ∼1 MDa (Fig. 6 *A* and *B*, *Left*) and a substantial amount sedimented in the >25S region, migrating in the blue native gel at >1 MDa (Fig. 6*A*, *Left*). The high molecular weight material was sensitive to RNase as were the REH1-containing RECC materials in fractions 10–13 (Fig. 6*A*, *Right*). This can also be seen in SDS gels of the same gradient fractions (Fig. 6*B*). The RNase-sensitive high molecular weight material is reminiscent of the previously reported RECC* particles that bound substoichiometric amounts of several other editing complexes (4). This evidence suggests that a portion of the tagged REH1 protein is associated with the RECC* particles via RNA linkers.

Additional evidence for an association of REH1 with the RECC was obtained by TAP purification, performed with or without RNase pretreatment (Fig. 6*C*). The REL1/REL2 internal RECC proteins and the MRP1/2 proteins were detected by Western analysis in the pull-down prior to RNase treatment but not after such treatment (Fig. 6*C*, *Right*). The coprecipitated REL1 and REH1 proteins were in substoichiometric amounts because they could not be visualized in the SDS gel by Sypro staining (Fig. 6*C*, *Left*). The three visible Sypro-stained bands in the REH1 TAP pull-down were identified by mass spectrometry as the SPB-tagged REH1 (II), a 10-kDa REH1 C-terminal breakdown product (III), and a 70-kD band (I) containing two contaminating proteins: TEV protease and a cytosolic DEAD-box protein (Fig. 6*C* and Table S3). The presence of this cytosolic helicase in the REH1-TAP pull-down should be investigated further.

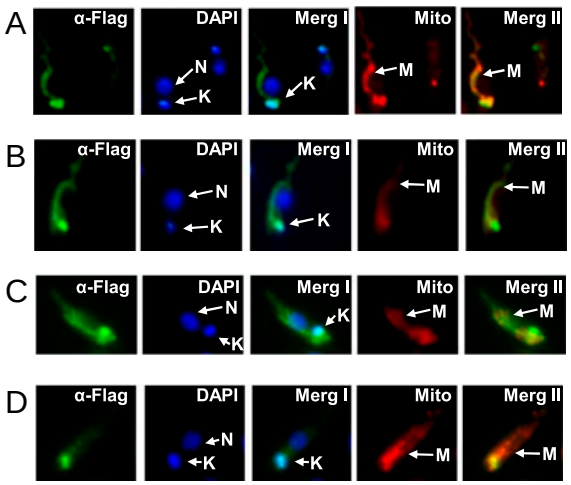

Fig. 5. Intracellular localization in late log phase *L. tarentolae* of SAP-tagged Lm REH1, TAP-tagged REL1, and the S17 and L3 TAP-tagged kinetoplast ribosome proteins. (*A*) Representative cells expressing SAP-tagged REH1. Cells were stained with mouse anti-FLAG antibody + Alexa Fluor 488 conjugated F(ab) fragment (α-FLAG, green) to visualize the SAP-tagged REH1. DAPI was used to visualize the nucleus and kinetoplast, and MitoTracker CMXRos was used to visualize the entire mitochondrion. A merge of the FLAG and DAPI panels is shown as MergI and a merge of the FLAG and MitoTracker panels is shown as MergII. N: nucleus, K: kinetoplast, M: mitochondrion. (*B*) Representative cell expressing TAP-tagged REL1. See legend in *A* for details. Images of entire fields are shown in Fig. S6. (*C*) A cell expressing TAP-tagged mitochondrial ribosomal protein S17. (*D*) A cell expressing TAP-tagged mitochondrial ribosomal protein L3.

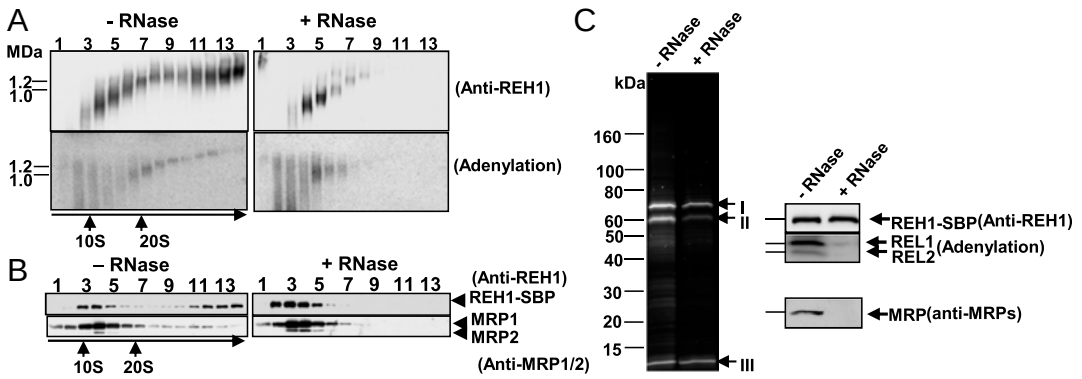

Fig. 6. RNA-dependent association of REH1 with the RECC. (*A*) Clarified lysate from *L. tarentolae* cells expressing SAP-tagged REH1 was bound to IgG-Sepharose and the SBP-tagged REH1 released with TEV protease. Half was treated with RNase A (0.1 mg/mL). After glycerol gradient sedimentation, fractions were run in blue native gels, which were blotted and probed with anti-REH1. Aliquots of fractions were also autoadenylated with $\alpha[^{32}P]$ATP to label the REL1 RECC protein prior to blue native gel analysis. These gels were dried and exposed to a phosphoimager screen. (*B*) Gradient fractions from *A* were run in SDS gels, which were blotted and probed with anti-REH1 or anti-MRP1/2. (*C*) The TEV-released material in *A*, with or without RNase treatment, was bound to streptavidin–Sepharose and the SBP-tagged REH1 released with 2 mM biotin. The SBP-tagged REH1 was run in SDS gels, which were autoadenylated and stained with Sypro (Invitrogen), or blotted and probed with anti-REH1 or anti-MRP1/2. Note that the labeled REL1/REL2 and the MRP1/2 proteins were detected only prior to RNase treatment. The three major stained bands were subjected to mass spectrometry (data shown in Table S3).

Discussion

REH1 is essential as shown by the growth phenotype caused by down-regulation of REH1 expression. The partial growth inhibition could be due to incomplete down-regulation, a slow turnover of the protein or an enzyme redundancy. Down-regulation also causes a decrease in abundance of edited mRNAs for the six genes assayed, with editing of the A6 and CR3 mRNAs being the most affected. Possible roles of the REH1 helicase in RNA editing are (*i*) to directly assist in the processive editing reaction itself within a single gRNA-mediated block as editing proceeds from site to site or (*ii*) to be involved in gRNA displacement between adjacent editing blocks. Model 1 is ruled out by the observed lack of effect of REH1 down-regulation on intrablock editing. Model 2 is supported by the significant decrease in the relative abundance of mRNAs edited in two or more adjacent blocks by REH1 down-regulation as compared to those edited in a single block, and by the accumulation of the gRNA/block 1 edited A6 mRNA duplex. These data suggest that REH1 is involved with the progression of editing from one gRNA-mediated editing block to the next adjacent upstream block.

The mechanism of this involvement, however, is not clear. The fact that recombinant REH1 protein has gRNA/mRNA duplex unwinding activity in vitro may suggest an in vivo role in directly unwinding the mRNA/gRNA duplex formed by the editing of all the sites mediated by a single gRNA and liberating an edited mRNA single strand available for hybridization of the adjacent gRNA. However, in the case of REH1, the evidence does not distinguish between a direct effect on unwinding of the gRNA/mRNA duplex or an indirect effect, such as described for eIF4AIII, a core component of the exon junction complex, and some putative RNA helicases that are involved in snoRNA release from preribosomes (27–31). Another potential function of REH1 could be to unwind *cis* elements within the preedited mRNA. A dominant-negative mutation of REH1 and ectopic reexpression of wild-type REH1 might indeed help to explore the role of REH1 in vivo. In fact, the evidence that the largest effect of REH1 down-regulation on editing is on the pan-edited A6 and CR3 mRNAs suggests that the in vivo activity of REH1 is substrate-specific and perhaps is regulated by transient binding of cofactors. Along this line, no detectable in vitro unwinding activity had been observed with *T. brucei* gradient fractions that showed a peak of Hel61 (REH1) by blot analysis (21) nor in the Lm REH1 SAP pull-down (Fig. S7*B*). These data suggest the possibility of regulation of helicase activity in vivo.

There have been conflicting reports on the association of REH1 with the RECC. Tb REH1 was detected by mass spectrometry analysis in an MP63-immunoprecipitated sample and also in a RECC preparation isolated by ion-exchange chromatography (32–34). However, REH1 was not detected in REN1-, REN2-, or REN3-TAP pull-downs from *T. brucei* (32, 35), nor in REL1-TAP and MP44-TAP pull-downs from *L. tarentolae* (7, 11). These results could be explained by our finding that REH1 is associated with the RECC by RNA linkers, as are several other editing-associated complexes (6, 11), and that this linkage is easily disrupted during the isolation.

Immunofluorescence of REH1 showed a concentration in the kinetoplast DNA (kDNA) region of the mitochondrion. Interestingly, the REL1 RNA ligase, a component of the RECC, and the S17 and L3 kinetoplast ribosome proteins also exhibited a concentration in the kDNA region of the mitochondrion, suggesting the intriguing possibility of a physical linkage of kDNA transcription, translation, and editing pathways, but this remains to be investigated. Our localization results differ somewhat from several previous studies that showed that editing proteins are distributed throughout the mitochondrion with no apparent concentration (36, 37) and that the RNA-linked editing proteins, GAP1 and GAP2, are localized in discrete particles throughout the mitochondrion (14). These differences could be species-dependent or could be due to technical details.

More work is required to fully understand the precise role of the REH1 helicase in RNA editing, but it is clear from the results in this paper that REH1 is involved in the 3′ to 5′ polarity of editing in a multi-gRNA-mediated editing domain.

Materials and Methods

SI Text contains details of plasmid construction, real-time PCR, poisoned primer extension, purification of SAP-tagged Lm REH1, ATPase activity assay, immunofluorescent localization of REH1, REL1, S17, L3, and glutamate dehydrogenase, mitochondrial importation of L3-TAP and S17–TAP proteins, and sedimentation analysis of kinetoplast ribosomal complexes. The *SI Text* tables contain sequences of DNA primers and RNA oligonucleotides used in the assays, and sequences of peptides derived from protein bands in Fig. 3*C*

ACKNOWLEDGMENTS. We thank Bob Nelson for the original construction of the SAP vector in our laboratory, Kent Hill for use of a fluorescence microscope, Stephen Smale and Jian Xu for the use of a Real-Time PCR apparatus, and Agda Simpson and Kestrel Rogers for generation of antibodies. The antibody against Tb REH1 was provided by Ulrich Göringer (Technical University of Darmstadt, Darmstadt, Germany) and the 2913 strain of *T. brucei* was provided by George Cross (Rockfeller University, New York). We thank David King for mass spectrometry of gel bands to identify proteins. This work was supported by National Institutes of Health Grant AI09102 (to L.S.).

1. Simpson L, Sbicego S, Aphasizhev R (2003) Uridine insertion/deletion RNA editing in trypanosome mitochondria: A complex business. *RNA* 9:265–276.
2. Stuart KD, Schnaufer A, Ernst NL, Panigrahi AK (2005) Complex management: RNA editing in trypanosomes. *Trends Biochem Sci* 30:97–105.
3. Blum B, Bakalara N, Simpson L (1990) A model for RNA editing in kinetoplastid mitochondria: "Guide" RNA molecules transcribed from maxicircle DNA provide the edited information. *Cell* 60:189–198.
4. Osato D, et al. (2009) Uridine insertion/deletion RNA editing in trypanosomatid mitochondria: In search of the editosome. *RNA* 15:1338–1344.
5. Simpson L, Aphasizhev R, Lukes J, Cruz-Reyes J (2010) Guide to the nomenclature of kinetoplastid RNA editing: A proposal. *Protist* 161:2–6.
6. Aphasizhev R, et al. (2003) Isolation of a U-insertion/deletion editing complex from Leishmania tarentolae mitochondria. *EMBO J* 22:913–924.
7. Li F, et al. (2009) Structure of the core editing complex (L-complex) involved in uridine insertion/deletion RNA editing in trypanosomatid mitochondria. *Proc Natl Acad Sci USA* 106:12306–12310.
8. Simpson L, Aphasizhev R, Gao G, Kang X (2004) Mitochondrial proteins and complexes in Leishmania and Trypanosoma involved in U-insertion/deletion RNA editing. *RNA* 10:159–170.
9. Worthey EA, Schnaufer A, Mian IS, Stuart K, Salavati R (2003) Comparative analysis of editosome proteins in trypanosomatids. *Nucleic Acids Res* 31:6392–6408.
10. Golas MM, et al. (2009) Snapshots of the RNA editing machine in trypanosomes captured at different assembly stages *in vivo*. *EMBO J* 28:766–778.
11. Aphasizhev R, Aphasizheva I, Nelson RE, Simpson L (2003) A 100-kD complex of two RNA-binding proteins from mitochondria of Leishmania tarentolae catalyzes RNA annealing and interacts with several RNA editing components. *RNA* 9:62–76.
12. Schumacher MA, Karamooz E, Zikova A, Trantirek L, Lukes J (2006) Crystal structures of T. brucei MRP1/MRP2 guide-RNA binding complex reveal RNA matchmaking mechanism. *Cell* 126:701–711.
13. Weng J, et al. (2008) Guide RNA-binding complex from mitochondria of trypanosomatids. *Mol Cell* 32:198–209.
14. Hashimi H, Čičová Z, Novotná L, Wen YZ, Lukeš J (2009) Kinetoplastid guide RNA biogenesis is dependent on subunits of the mitochondrial RNA binding complex 1 and mitochondrial RNA polymerase. *RNA* 15:588–599.
15. Acestor N, Panigrahi AK, Carnes J, Zikova A, Stuart KD (2009) The MRB1 complex functions in kinetoplastid RNA processing. *RNA* 15:277–286.
16. Hernandez A, et al. (2010) REH2 RNA helicase in kinetoplastid mitochondria: Ribonucleoprotein complexes and essential motifs for unwinding and guide RNA (gRNA) binding. *J Biol Chem* 285:1220–1228.
17. Ochsenreiter T, Hajduk SL (2006) Alternative editing of cytochrome c oxidase III mRNA in trypanosome mitochondria generates protein diversity. *EMBO Rep* 7:1128–1133.
18. Feagin JE, Abraham J, Stuart K (1988) Extensive editing of the cytochrome c oxidase III transcript in Trypanosoma brucei. *Cell* 53:413–422.
19. Maslov DA, Simpson L (1992) The polarity of editing within a multiple gRNA-mediated domain is due to formation of anchors for upstream gRNAs by downstream editing. *Cell* 70:459–467.
20. Missel A, Goringer HU (1994) Trypanosoma brucei mitochondria contain RNA helicase activity. *Nucleic Acids Res* 22:4050–4056.
21. Missel A, Souza AE, Norskau G, Goringer HU (1997) Disruption of a gene encoding a novel mitochondrial DEAD-box protein in Trypanosoma brucei affects edited mRNAs. *Mol Cell Biol* 17:4895–4903.
22. Hong M, Simpson L (2003) Genomic organization of Trypanosoma brucei kinetoplast DNA minicircles. *Protist* 154:265–279.
23. Ochsenreiter T, Cipriano M, Hajduk SL (2007) KISS: The kinetoplastid RNA editing sequence search tool. *RNA* 13:1–4.
24. Puig O, et al. (2001) The tandem affinity purification (TAP) method: A general procedure of protein complex purification. *Methods* 24:218–229.
25. Cordin O, Banroques J, Tanner NK, Linder P (2006) The DEAD-box protein family of RNA helicases. *Gene* 367:17–37.
26. Peris M, et al. (1994) Characterization of two classes of ribonucleoprotein complexes possibly involved in RNA editing from Leishmania tarentolae mitochondria. *EMBO J* 13:1664–1672.
27. Andersen CB, et al. (2006) Structure of the exon junction core complex with a trapped DEAD-box ATPase bound to RNA. *Science* 313(5795):1968–1972.
28. Bono F, Ebert J, Lorentzen E, Conti E (2006) The crystal structure of the exon junction complex reveals how it maintains a stable grip on mRNA. *Cell* 126:713–725.
29. Kos M, Tollervey D (2005) The putative RNA helicase Dbp4p is required for release of the U14 snoRNA from preribosomes in saccharomyces cerevisiae. *Mol Cell* 20:53–64.
30. Liang XH, Fournier MJ (2006) The helicase Has1p is required for snoRNA release from pre-rRNA. *Mol Cell Biol* 26:7437–7450.
31. Bohnsack MT, Kos M, Tollervey D (2008) Quantitative analysis of snoRNA association with pre-ribosomes and release of snR30 by Rok1 helicase. *EMBO Rep* 9(12): 1230–1236.
32. Panigrahi AK, et al. (2006) Compositionally and functionally distinct editosomes in Trypanosoma brucei. *RNA* 12:1038–1049.
33. Panigrahi AK, Allen TE, Stuart K, Haynes PA, Gygi SP (2003) Mass spectrometric analysis of the editosome and other multiprotein complexes in Trypanosoma brucei. *J Am Soc Mass Spectr* 14:728–735.
34. Stuart K, Panigrahi AK, Schnaufer A (2004) Identification and characterization of trypanosome RNA-editing complex components. *Methods Mol Biol* 265:273–291.
35. Carnes J, Trotter JR, Peltan A, Fleck M, Stuart K (2008) RNA editing in Trypanosoma brucei requires three different editosomes. *Mol Cell Biol* 28:122–130.
36. Oberholzer M, Morand S, Kunz S, Seebeck T (2006) A vector series for rapid PCR-mediated C-terminal in situ tagging of Trypanosoma brucei genes. *Mol Biochem Parasitol* 145:117–120.
37. Panigrahi AK, et al. (2001) Association of two novel proteins, TbMP52 and TbMP48, with the Trypanosoma brucei RNA editing complex. *Mol Cell Biol* 21:380–389.

Supporting Information

Li et al. 10.1073/pnas.1014152108

SI Materials and Methods.

Construction of Plasmids. For conditional RNAi, a 500-bp fragment from the 5′ end of Tb REH1 was amplified with the primers shown in Table S1. The fragments were inserted into the pLew-HX-100-GFP vector using the HindIII, XbaI and NdeI, BamHI sites to form a head-to-head RNAi plasmid under poly (ADP-ribose) polymerase promoter control.

The REH1 gene was amplified from *Leishmania major* (Lm) genomic DNA with LmH1-F and LmH1-R primers. The full-length gene was cloned into pCR2.1-TOPO (Invitrogen).

For expression in *Leishmania tarentolae* with a streptavidin-binding motif (SBP) tag, the REH1 gene was excised with BamHI and XbaI and then cloned into the same sites of pX-derived pX-REL1-TAP vector. To replace the calmodulin binding peptide tag in the vector, the SBP tag (1) was amplified from the pBEn-SBP-SET1 plasmid (Stratagene) with SBP-F and SBP-R primers and was inserted into pX-REH1-TAP vector using XbaI and NheI.

For expression in the baculovirus system, the predicted mitochondrial targeting signal (positions 1–44) was removed by PCR amplification of pX-REH1-SBP with primers LmH1-BV-F and LmH1-BV-R. The fragment which contains SBP tagged REH1 was inserted into the pFastBac1 vector (Invitrogen) with BamHI and NotI. Expression of proteins in baculovirus transfected Sf9 insect cells was carried out as described by the company.

For expression in *Escherichia coli*, the REH1 gene was amplified with primers, LmH1-Ec-F and LmH1-Ec-R, and the product was inserted into pET28a (Novagene) vector with NdeI and EcoRI. HT-tagged REH1 was purified by metal affinity chromatography on Talon resin (BD Biosciences) according to the manufacturer's protocol. Polyclonal antibodies were raised against the purified *E. coli* expressed recombinant REH1 (Covance).

The coding regions of mitochondrial ribosomal proteins S17 from *L. major* and L3 from *L. tarentolae* were amplified using oligonucleotide primers derived from the corresponding *L. major* sequences (S17: LmjF35.3850 and L3: LmjF29.0030). The S17 primers were DM6845, 5′-GGG*GGATCC*ATGTTTCGTCAGTCGCTTCTTCGACTCA (BamHI site italicized), and DM6846, 5′-CAT*TCTAGA*AGGCGACTTCTTCAAGTTTTTGAAGTCATAC (XbaI site italicized). The L3 primers were: DM6847, 5′-GGG*GGATCC*ATGCATCGTTTCCGTGTGTGTGCGCTCGGCG, and DM6848, 5′-CAT*TCTAGA*CGTCTTGACGCGCTTATATTTCAGAATCTTTG. The amplified DNA fragments were digested with BamHI and XbaI and cloned into pX-RET2-TAP vector in *E. coli* using standard procedures. The selected recombinant plasmids expressing S17-TAP and L3-TAP fusions were used to transfect *L. tarentolae*. Mitochondrial importation and cosedimentation of the TAP-tagged proteins with the 45S–50S ribosomal complexes was confirmed in both cases.

Real-Time PCR Analysis. Total RNA was isolated from cells grown in the presence or absence of tetracycline with Tri reagent as described by the manufacturer (MRC). Twelve micrograms of total RNA were treated with DNase I (Ambion). The cDNA templates were reverse transcribed from 4.5 μg of RNA using random hexamers and Taqman reverse transcription reagents (Applied Biosystems) in a 30-μL reaction. The templates were diluted eightfold in water. For each PCR reaction, 2.5-μL cDNA template (or −RT control), 5 μL of 1.5 μM forward primer, 5 μL of 1.5 μM reverse primer, and 12.5 μL of SYBR Green Master Mix (Applied Biosystems) were combined in a well of a 96-well plate (Denville Inc.). The PCR amplification conditions were 95 °C (10 min) and 45 cycles of 95 °C (15 s), 55 °C (30 s), and 63 °C (30 s). The amplification was performed in triplicate. The sequences of primers for each preedited and edited mRNA can be found in Table S1.

RNase Protection and Poisoned Primer Extension. Total RNA was isolated with the Tri Reagent (MRC) as described in the manufacturer's protocol, and contaminating DNA was eliminated with DNase (Ambion). About 35 μg RNA was treated with 0.5–1 U RNase One (Promega) in 100 μL of 10 mM Tris pH7.5, 5 mM EDTA, 200 mM NaOAC buffer for 1 h at 10 °C and SDS was added to a final concentration of 0.1% to deactivate RNase One. 5'-32P-end labeled oligonucleotides (0.25 pmol) were coprecipitated with residual RNA and dissolved in 10 μL of 30 mM Hepes pH 7.5, 100 mM KOAC, 0.1 mM EDTA for annealing. Primer extension was carried out as described previously (2).

Samples were heated for 2 min at 90 °C and cooled down to 37 °C for 1 h. Twenty microliters of extension solution prewarmed to 37 °C were quickly added to the hybridization mix. The final reaction mixture contains 50 mM Tris-HCl pH 8.3, 50 mM KCl, 10 mM $MgCl_2$, 0.5 mM spermidine, 10 mM DTT, 200 μM *d*(ATP,GTP,TTP)/ddCTP, and 5 U of avian myeloblastosis virus reverse transcriptase (Promega). Upon extension at 37 °C for 30 min, RNA was hydrolyzed by adding 1.5 μL of 0.5 M EDTA and 3.2 μL of freshly made 2 M NaOH, and incubating at 65 °C for 30 min. Reaction mix was neutralized by 4 μL of freshly made 2 M HCl. Extension products were precipitated with 1 μg/reaction of glycogen (Ambion) and 3 V of ethanol, washed with 90% ethanol, and resuspended in 5 μL in 95% formamide, 10 mM EDTA, 0.05% xylene cyanol, 0.05% bromphenol blue loading buffer. Products were analyzed on 10% polyacrylamide/8M Urea gel.

Purification of SAP-Tagged Recombinant Lm REH1. Insect Sf9 cells (2 g) were resuspended in 12 mL TMK buffer (20 mM Tris-HCl, pH7.6, 60 mM KCl, 10 mM $MgCl_2$) with 0.5% NP-40 and one tablet of Complete Protease Inhibitors (Roche). After lysis on ice for 30 min, the lysate was sonicated 3 times for 20 s. The lysate was cleared by centrifugation at 200,000 × *g* for 20 min. The supernatant was incubated with 0.5 mL IgG Sepharose FF (GE Healthcare) for 3 h in the cold room and transferred to a disposable 5-mL column. The beads were washed sequentially with 30 mL of TMK buffer plus 0.1% NP-40 and 10 mL of TEV-protease buffer (TMK buffer plus 0.1% NP-40 and 1 mM DTT). Four microliters of the same buffer with 100 U of TEV proteinase were added to the column and the column was incubated overnight with constant mixing. The IgG resin was drained and washed with 2 mL of TMK buffer plus 0.1% NP-40. The eluted material was pooled and applied to a Mono S 5/50 GL FPLC column (Amersham Biosciences) previously equilibrated with the same buffer. The column was eluted with a gradient of NaCl (0–0.6 M) in the same buffer. The fractions containing ATPase activity were pooled and incubated with 0.3 mL of streptavidin sepharose (GE Healthcare) for 1 h in the cold room and transferred to a disposable 5-mL column. The beads were washed with 20 mL of 20 mM Hepes-KOH pH 7.6, 60 mM KCl, 2.5 mM $MgCl_2$, 1 mM DTT, and 0.1% NP-40, and then the bound proteins were eluted with 3 mL of 20 mM Hepes-KOH pH7.6, 60 mM KCl, 2.5 mM $MgCl_2$, 1 mM DTT , 2 mM biotin, and 0.1% NP-40.

ATPase Activity Assay. ATPase reactions were carried out as described (3) with minor modifications. A typical ATPase assay was carried out in a 40-μL reaction volume containing 50 mM Hepes-KOH pH 8.2, 2.5 mM $MgCl_2$ and 2 mM ATP, 2 μg of appropriate RNA and 5 μL of recombinant REH1 helicase. The reaction mixture was incubated at 27 °C for 30 min in a 96-well plate. Then the reaction was terminated by addition of 160 μL of a malachite green/molybdate/polyvinyl alcohol acidic solution. The absorption at 630 nm was measured and the ATPase activity was calculated as the amount of Pi produced through hydrolysis of ATP using a standard curve constructed using known concentrations of potassium dihydrogen phosphate.

Unwinding Assay. In brief, 20 μL reaction mixture contained 10 mM Hepes pH 7.5, 60 mM KCl, 2.5 mM $MgCl_2$, 2 mM DTT, 2 mM ATP, 5% glycerol, 60 μg/mL BSA, 400 units/mL RNase guard, 2.5 nM dsRNA, and 2 μL SBP-tagged rREH1. Reactions were incubated at 27 °C for 60 min then stopped by adding 5 μL of a solution containing 50% glycerol, 2% SDS, 20 mM EDTA, 0.01% bromphenol blue, and xylene cyanol dyes. Samples were separated by 15% nondenaturing PAGE.

Immunofluorescent Localization of REH1, REL1, S17, L3, and Glutamate Dehydrogenase. *L. tarentolae* (2×10^7) cells expressing TAP/SAP-tagged proteins were harvested and resuspended in Brain Heart Infusion Medium with 0.4 μM MitoTracker CMXRos (Invitrogen), and the cells were incubated at 27 °C for 30 min and washed with PBS. Then the cells were fixed in 4% paraformaldehyde in PBS for 5 min and fixation was stopped by two 5-min washes in 0.1 M glycine in PBS. The cells were allowed to adhere to poly-L-lysine-coated glass slides for 30 min, followed by incubation for 10 min in 0.025% Triton X-100 in PBS. The slides were kept in methanol at −20 °C overnight and rehydrated by three washes in PBS for 5 min each. The cells were then blocked in 20% goat serum in PBST (0.05% Tween-20 in PBS) at room temperature for 2 h, followed by a 60-min incubation with anti-FLAG monoclonal antibody at a 1:100 dilution (Trend Phara & Tech). After three times washing in PBST, cells were incubated further with $F(ab)_2$ fragment of goat anti-mouse IgG conjugated with Alexa Fluor 488 (Invitrogen) at a 1:500 dilution for 60 min. The slides were washed again three times for 5 min each in PBST and were mounted by using ProLong Gold antifade reagent with DAPI (Invitrogen), which stains both the nucleus and the kinetoplast. For fluorescence microscopy, cells were imaged by using a Zeiss Axioskop II compound microscope with a 63× Plan-neofluor oil-immersion objective lens, and images were captured by using a Zeiss Axiocam digital camera and Zeiss Axiovision 4.5 software. Red, blue, green, and phase-contrast images of the same field were captured independently and were merged using Adobe Photoshop. The same procedure was used to detect immunofluorescence of the endogenous mitochondrial glutamate dehydrogenase using a polyclonal antibody against this protein.

Mitochondrial Importation of L3-TAP and S17-TAP Fusions. The transfected cell lines of *L. tarentolae* were propagated as 200-mL cultures to a density of 10^8 cells/mL. Cells were completely ruptured using the Stansted homogenizer and a crude mitochondrial pellet obtained as described previously (4). The pellet was resuspended in 2 mL of SHE (0.25 M sorbitol, 20 mM Hepes, and 2 mM EDTA, pH 7.5) buffer solution. The supernatant, representing the cytosolic fraction, was concentrated using the Amicon Ultra-15 Centrifugal Filter Unit to the volume of 2 mL. An equal volume representing each fraction and an equivalent amount of a total cell lysate were analyzed in a 8–16% polyacrylamide Tris-glycine SDS Novex® gel (Invitrogen). Western blots were probed for the TAP moiety present in the fusions with the PAP reagent (Sigma) followed by ECL detection (SuperSignal® West Pico substrate kit, Thermo Scientific).

Sedimentation Analysis of Mitochondrial Ribosomal Complexes from *L. tarentolae*. The *L. tarentolae* cell lines expressing L3-TAP and S17-TAP fusions were used to isolate mitochondria, followed by velocity sedimentation of ribosomal complexes from a dodecyl maltoside lysate of mitochondria in a 7–30% sucrose gradient as described previously (5). Gradient fractions were assayed for presence and relative quantity of the 9S and 12S ribosomal RNA (5), as well as for the TAP-tagged proteins by probing Western blots of electrophoretic gels with the PAP reagent.

1. Keefe AD, Wilson DS, Seelig B, Szostak JW (2001) One-step purification of recombinant proteins using a nanomolar-affinity streptavidin-binding peptide, the SBP-tag. *Protein Expr Purif* 23:440–446.
2. Etheridge RD, Aphasizheva I, Gershon PD, Aphasizhev R (2008) 3' adenylation determines mRNA abundance and monitors completion of RNA editing in T. brucei mitochondria. *EMBO J* 27:1596–1608.
3. Chan KM, Delfert D, Junger KD (1986) A direct colorimetric assay for Ca2+ -stimulated ATPase activity. *Anal Biochem* 157:375–380.
4. Connell GJ, Byrne EM, Simpson L (1997) Guide RNA-independent and guide RNA-dependent uridine insertion into cytochrome *b* mRNA in a mitochondrial lysate from *Leishmania tarentolae*—Role of RNA secondary structure. *J Biol Chem* 272:4212–4218.
5. Maslov DA, et al. (2006) Isolation and characterization of mitochondrial ribosomes and ribosomal subunits from *Leishmania tarentolae*. *Mol Biochem Parasitol* 148:69–78.

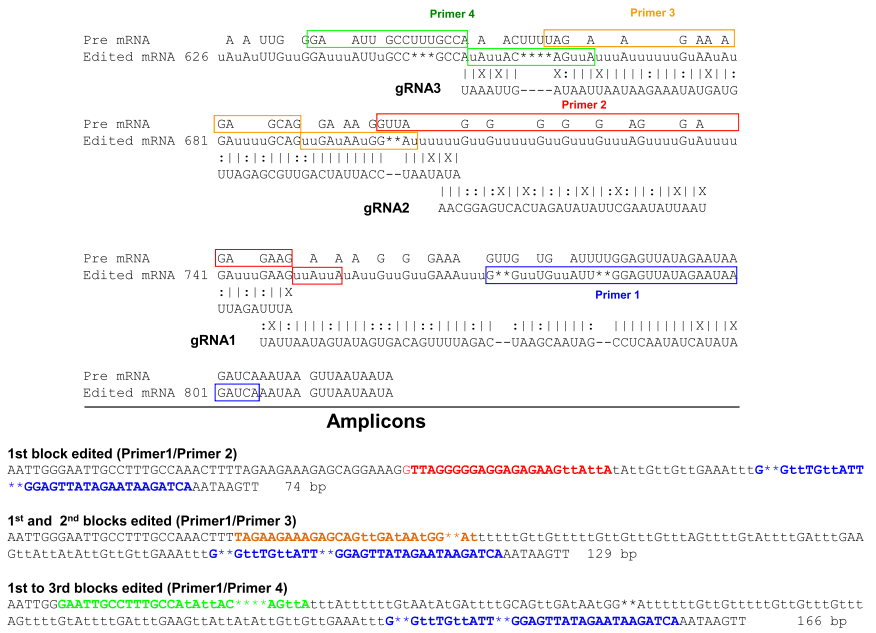

Fig. S1. Real-time RT-PCR analysis of partially edited *Trypanosoma brucei* ATPase subunit 6 mRNA. (*Upper*) Diagram of A6 mRNA and gRNA sequences. The PCR primers are indicated by boxed sequences. The gRNAs 1–3 are indicated. |, Watson–Crick base pairs. :, G-U base pairs. (*Lower*) Sequences of the amplicons obtained. The editing blocks are indicated by color. Editing block 1 = primer 1 + primer 2. Editing blocks 1 + 2 = primer 1 + primer 3. Editing blocks 1 + 2 + 3 = primer 1 + primer 4.

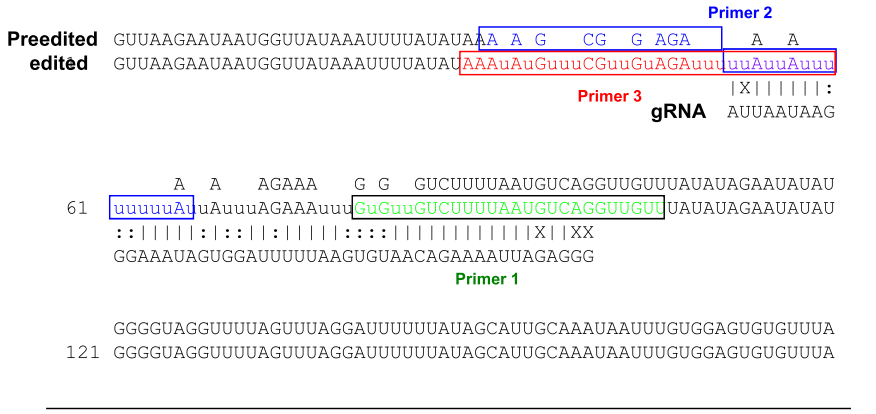

Amplicons

1st gRNA edited block (Primer1/Primer 2)

GGUUAUAAAUUUUAUAUAAAAGCGGAGAuuAuuAuuuuuuuuuAuuAuuuAGAAAuuuGuGuuGUCUUU
UAAUGUCAGGUUGUUUAUAUAGAAUAUAUGGGGUAGGUUUUAGUUUAGGAU 65 nt

1st+2nd gRNAs edited block (Primer 1/Primer 3)

GGUUAUAAAUUUUAUAUAAAuAuGuuuCGuuGuAGAuuuuuAuuAuuuuuuuuAuuAuuuAGAAAuuu
GuGuuGUCUUUUAAUGUCAGGUUGUUUAUAUAGAAUAUAUGGGGUAGGUUUUAGUUUAGGAU 77

Fig. S2. Real-Time RT-PCR analysis of partially edited *T. brucei* cytochrome b mRNA. (*Upper*) Diagram of mRNA and gRNA sequences. The PCR primers are indicated by boxed sequences. The gRNA is indicated. |, Watson–Crick base pairs. :, G-U base pairs. (*Lower*) Sequences of the amplicons obtained. The editing blocks are indicated by color. Editing block 1 = primer 1 + primer 2. Editing blocks 1 + 2 = primer 1 + primer 3.

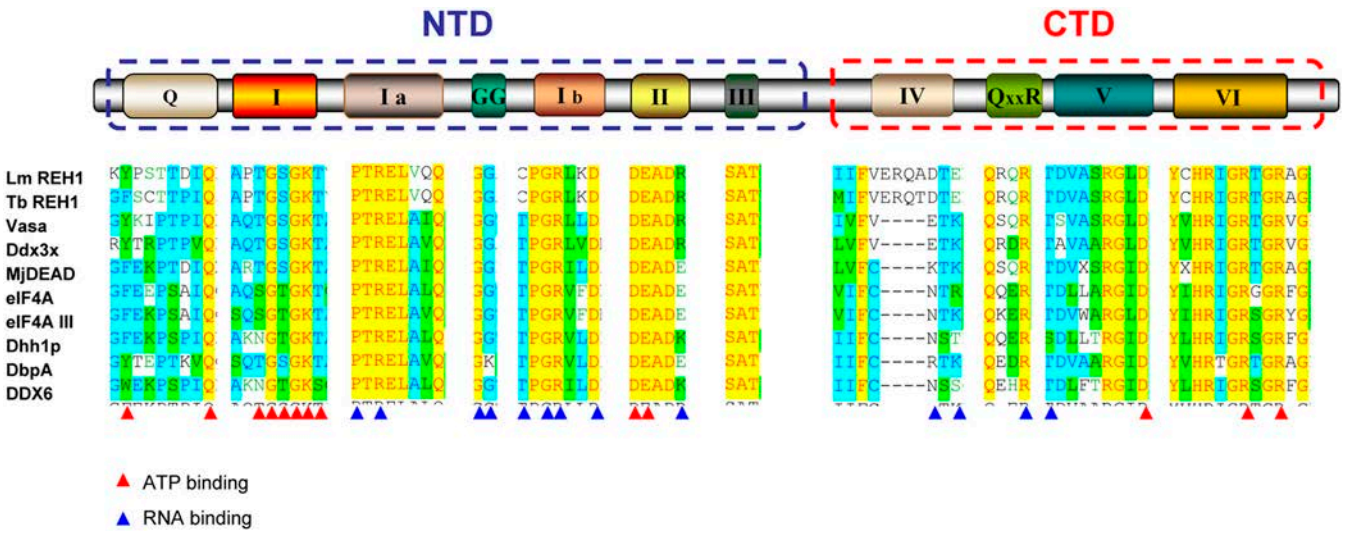

Fig. S3. Alignment of conserved motifs of Lm REH1 and other RNA helicases. Sequences of the conserved motifs from Lm REH1 (*Leishmania major*), Tb REH1 (*Trypanosoma brucei*), Vasa (*Drosophila Melanogaster*), Ddx3x (*Homo sapiens*), MjDEAD (*Methanocaldococcus jannaschii*), eIF4A (*Saccharomyces Cerevisiae*), eIF4A III (*Homo sapiens*), Dhh1p (*Saccharomyces Cerevisiae*), DbpA (*Bacillus subtilis*), and DDX6 (*Homo sapiens*). Matches are shown in black highlight and conserved changes in gray. Performed using Vector NTI (Invitrogen). NTD is N-terminal domain. CTD is C-terminal domain.

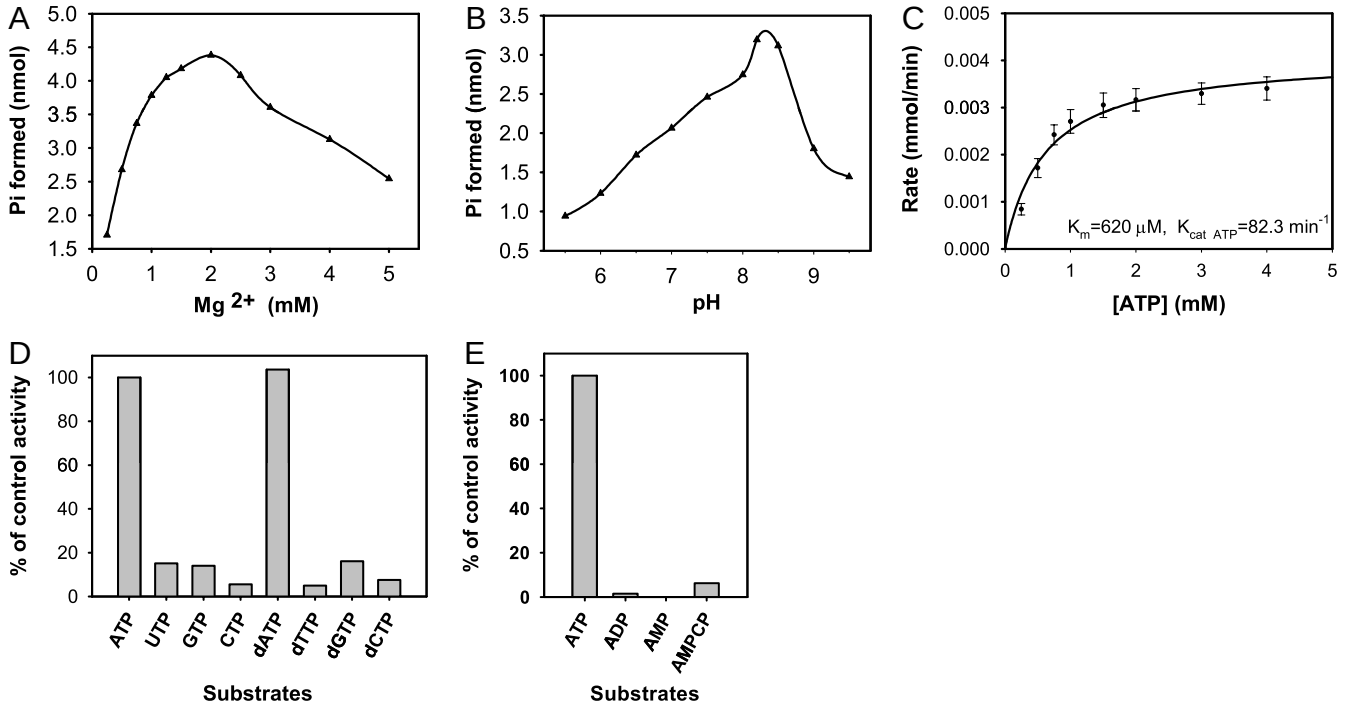

Fig. S4. Biochemical characterization of recombinant REH1. (*A*) The optimal concentration of $MgCl_2$ was determined in 50 mM of Hepes-KOH (pH 8.2) with 2 mM ATP. (*B*) The optimal pH was determined with 2 mM ATP and 2.5 mM $MgCl_2$. (*C*) Kinetic analysis of ATPase activity of purified tagged Lm Hel61. The reaction was performed in 50 mM of Hepes-KOH pH 8.2, 2 mM $MgCl_2$, 2 μg of poly U, and various concentrations of ATP. The solid line represents a Michaelis–Menton nonlinear curve fit to the data points (Sigmaplot). Error bars indicate one standard deviation. (*D*). Extent of hydrolysis of NTPs and dNTPs assayed in 50 mM of Hepes-KOH (pH 8.2) with 2.5 mM $MgCl_2$, 2 μg of poly U, and 2 mM of each NTP or dNTP. Activity is represented as percentage of ATP-hydrolysis activity. (*E*). ADP and AMP and also adenosine methylene diphosphate (AMPCP), a nonhydrolysable ATP analog, were used as substrates with purified rREH1 under same conditions as in *D*.

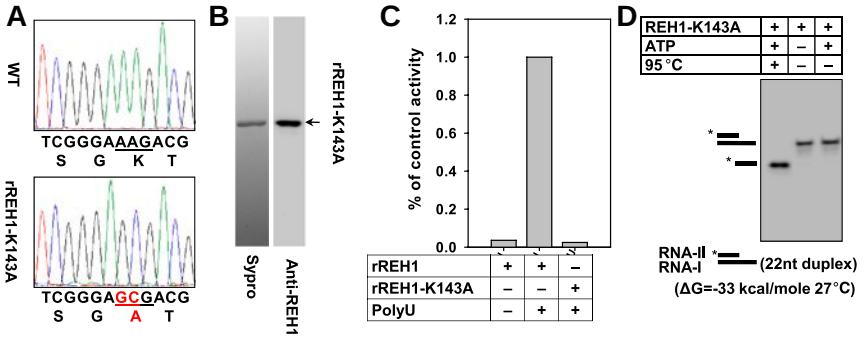

Fig. S5. Activities of REH1-K143A mutant. (*A*) The gene sequence of wild-type and K143A mutation of REH1. (*B*) Purification of rREH1-K143A protein. SDS gel stained with Sypro. Blots probed with anti-REH1 antibody. (*C*) ATPase activity of purified REH1-K143A mutant protein. The ATPase reactions were performed with or without poly U RNA. (*D*). Unwinding activity of REH1-K143A mutant. The reaction was performed with 10 nM rREH1-K143A and a RNA substrate with a 22-bp duplex with 15 nt 5′ overhang. The ^{32}P-labeled end is indicated by * in the diagram.

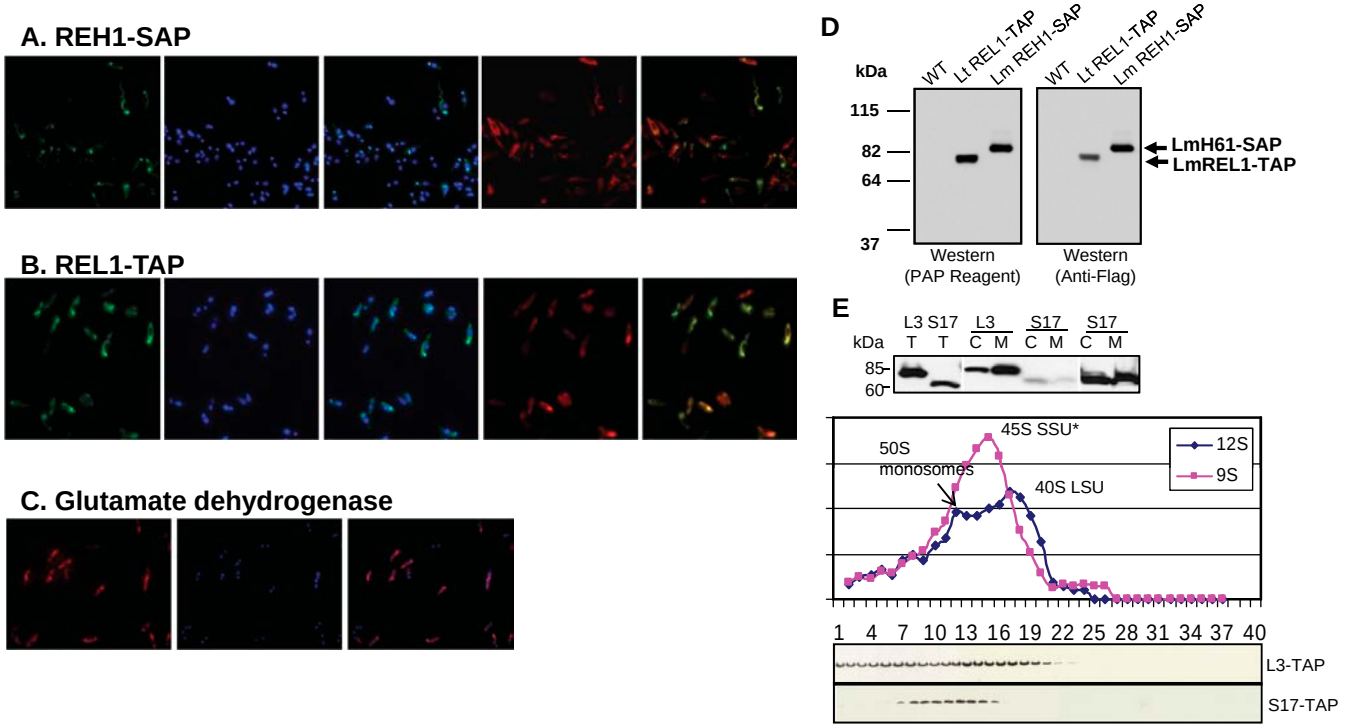

Fig. S6. Localization of mitochondrial proteins in *L. tarentolae*. (*A*) Immunolocalization of SAP-tagged Lm REH1 and (*B*) TAP-tagged Lt REL1 in late log phase *L. tarentolae* cells. Multiple layers of the same microscope field are shown. Green, cells stained with mouse anti-FLAG antibody and the *F*(ab) fragment of goat anti-mouse IgG conjugated with Alexa Fluor 488. Blue, cells stained with DAPI. Red, cells stained with MitoTracker CMXRos. The third panel in each set represents a merged image of DAPI-stained cells and antibody-stained cells. The last panel in each set represents a merged image of the MitoTracker-stained cells and the antibody-stained cells. (*C*) Immunolocalization of Lt glutamate dehydrogenase in late log phase *L. tarentolae* cells. Multiple layers of the same microscope field are shown. Red, cells stained with rabbit antiglutamate dehydrogenase antibody and the *F*(ab) fragment of goat anti-rabbit IgG conjugated with Alexa Fluor 594. Blue, cells stained with DAPI. The last panel represents a merged image of DAPI-stained cells and antibody-stained cells. (*D*) Specificity of anti-FLAG antibody. Cell extract from different cell lines were analyzed by SDS gel and PAP reagent and anti-FLAG (Trend Pharma & Tech) monoclonal antibody were used to detect the tagged proteins. (*E*) Cosedimentation with mitochondrial ribosomes of the L3-TAP and S17-TAP fusion proteins. (*Upper*) Cell lines of *L. tarentolae* expressing *L. tarentolae* L3-TAP (L3) and *L. major* S17-TAP (S17) were isotonically ruptured, and the cytosolic (C) and mitochondrial (M) fractions were separated by centrifugation. Proteins in each subcellular fraction were separated in a 8–16% polyacrylamide gel, followed by blotting, probing with the PAP reagent, and ECL detection. The proteins from a total cell lysate (T) were analyzed in parallel. The expected size of L3-TAP is 76 kDa and that of S17-TAP is 58 kDa (including the 22-kDa TAP moiety). With L3, most of the expressed protein was found in the mitochondrial fraction, whereas only a smaller fraction of the tagged S17 protein was imported. In addition, the overall expression level of S17 was lower than that observed with L3. Whether or not this can be attributed to the use of a heterologous S17 remains unknown. The two right-most lanes of the panel represent a longer exposure of the same blot. (*Lower*) Cosedimentation of TAP-tagged ribosomal proteins L3 and S17 with the mitochondrial ribosomal RNP complexes. (*Upper*) The typical relative quantity profile of the 9S small subunit and the 12S large subunit ribosomal RNAs in fractions of a sucrose gradient. In this case the profile represents the S17-TAP cell line. The 50S monosomes are detectable as a shoulder of a larger peak representing the small subunit-related 45S SSU* complex and a peak representing 40S large subunit (1–3). Sedimentation is from right to left. (*Lower*) Western blot analysis of proteins from fractions 2–38 of the sucrose gradients. Probing was done with the PAP reagent.

1. Maslov DA, et al. (2006) Isolation and characterization of mitochondrial ribosomes and ribosomal subunits from *Leishmania tarentolae*. *Mol Biochem Parasitol* 148:69–78.
2. Maslov DA, et al. (2007) Proteomics and electron microscopic characterization of the unusual mitochondrial ribosome-related 45S complex in Leishmania tarentolae. *Mol Biochem Parasitol* 152:203–12.
3. Sharma MR, et al. (2009) Structure of a mitochondrial ribosome with minimal RNA. *Proc Natl Acad Sci USA* 106:9637–42.

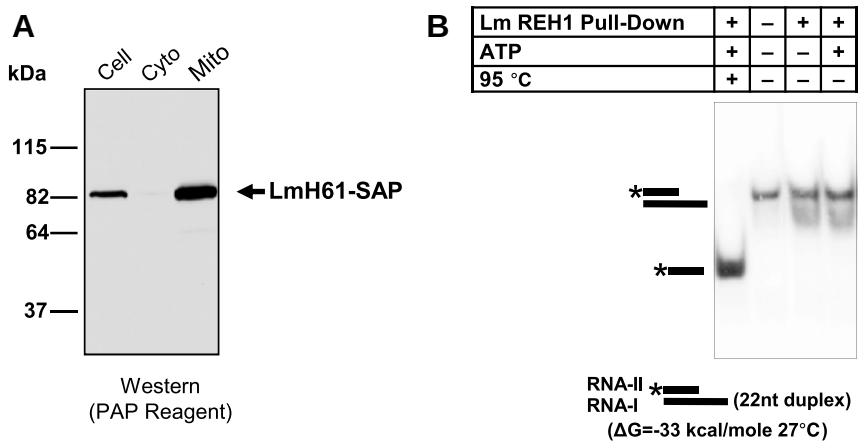

Fig. S7. Absence of unwinding activity of Lm REH1-SAP pull-down. (*A*) Expression of SAP-tagged Lm REH1 and mitochondrial importation. Equivalent amounts of whole cell, cytosol (*Cyto*) and mitochondrial extract (*Mito*) were separated in an 8–16% polyacrylamide SDS gel. The gel was blotted and probed with the peroxidase antiperoxidase (PAP) reagent (Sigma) to detect the SAP-tagged Lm REH1. (*B*) Model gRNA/mRNA substrate with a 22-bp duplex and a 15-nt 5′ overhang. The ^{32}P-labeled end is indicated by * in the diagram. Concentration of SAP pull-down in lanes 1, 3, 4 was 10 nm. The REH1-SAP pull-down was obtained as described in "Purification of SAP-tagged recombinant Lm REH1" but without MonoS chromatography.

Table S1. DNA oligonucleotides

Name	Sequence	Polarity	Application	Amplicon size, bp
		Cloning		
LmH1-F	CTATCGGATCCATGCGGCGTTTTGCAAGTGC	sense	LmREH1 PCR pX-LmH1-SAP	
LmH1-R	ACACCGTCTAGATGACCAGTCCAACGTGGACG	antisense		
SBP-F	GCATCTAGAATGGACGAGAAGACCACCG	sense	SBP tag PCR pX-LmH1-SAP	
SBP-R	CAGGCTAGCAGATCCACGCGGAACCAG	antisense		
LmH1-BV-F	AGTCCAGGATCCATGGAGGGATTGGCCCCCGCAA	sense	LmREH1 PCR pFb-LmH1-SAP	
LmH1-BV-R	GAATCGCGGCCGCTCTAGTTATTTATC	antisense		
LmH1-Ec-F	AGGTCGCATATGGAGGGATTGGCCCCCGCAA	sense	LmREH1 PCRpET28a-LmH1	
LmH1-Ec-R	ACAGTCGAATTCTTACCAGTVVAACGTGGACG	antisense		
TbH1i-F1	AAGCTTATGAGGGCCCTGCGTTGTGTTAGG	sense	TbREH1 PCR pLew100-TbH1i	
TbH1i-R1	TCTAGACCCGAACCTGTAGGAGCCAG	antisense		
TbH1i-F2	CATATGCCCGAACCTGTAGGAGCCAG	sense		
TbH1i-R2	GGATCCATGAGGGCCCTGCGTTGTGTTAGG	antisense		
		Real-Time-qPCR		
ND8P-F	GATTTTTGCCAACGCATTCAGGA	sense	ND8 pre PCR	82
ND8P-R	TCCCCTTCTCCCCTTCTCTC	antisense		
ND8E-F	GGATGTTCGTGTTGGGTGGA	sense	ND8 edit PCR	142
ND8E-R	ACACATAACAATCAATGAATGCGTAA	antisense		
ND9P-F	TAGGAGGATGATTGGGTAGCG	sense	ND9 pre PCR	134
ND9P-R	ATTAAGGTTGCCCTGTTGTCG	antisense		
ND9E-F	GTTGGAACGCGAATGTTTTGA	sense	ND9 edit PCR	156
ND9E-R	TCCACCAACACACAAAATAACAATACA	antisense		
ND7P-F*	GCGGGCGGAGCATTATT	sense	ND7 pre PCR	108
ND7P-R	ATTTCAAACAATCCTCAATAACCAA	antisense		
ND7E-F*	GCATCCCGCAGCACATG	sense	ND7 edit PCR	101
ND7E-R*	CTGTACCACGATGCAAATAACCTATAAT	antisense		
COIIIP-F*	GAAACCAGATGAGATTGTTTGCA	sense	COIII pre PCR	153
COIIIP-R*	TTCATTCCAACTAAACCCTTTCC	antisense		
COIIIE-F*	TTGTGTTTTATTACGTTGTATCCAGTATTG	sense	COIII edit PCR	128
COIIIE-R*	CGAAAGCAAACTCACAACACAAA	antisense		
CybP-F*	ATATAAAAGCGGAGAAAAAAGAAAG	sense	Cyb pre PCR	64
CybP-R*	CCCATATATTCTATATAAACAACCTGACA	antisense		
CybE-F*	AAATATGTTTCGTTGTAGATTTTTATTATTT	sense	Cyb edit PCR	94
CybE-R*	CCCATATATTCTATATAAACAACCTGACA	antisense		
A6P-F*	TTGCCTTTGCCAAACTTTTAGAAG	sense	A6 pre PCR	90
A6P-R*	ATTCTATAACTCCAAAATCACAACTTTCC	antisense		
A6E-F*	GATTTATTTTGGTTGCGTTTGTTATTATG	sense	A6 edit PCR	144
A6E-R*	CAAACCAACAAACAAATACAAATCAAAC	antisense		
CR3P-F	GACAGAGGGTTTATTTTTGAGGAT	sense	CR3 pre PCR	79
CR3P-R	AATAACGAAACTTTTCTTATGTCCTTC	antisense		

Name	Sequence	Polarity	Application	
CR3E-F	AATGTTTGATTGTTTGGTTTTGTTGTT	sense	CR3 edit PCR	162
CR3E-R	AAAAATAAACACAACAATAAACCCATAT	antisense		
COIIP-F*	ATTACAGTGTAACCATGTATTGACATT	sense	COII pre PCR	135
COIIP-R*	TTCATTACACCTACCAGGTTCTCT	antisense		
COIIE-F*	ATTACAGTGTAACCATGTATTGACATT	sense	COII edit PCR	141
COIIE-R*	ATTTCATTACACCTACCAGGTATACAA	antisense		
Murf2P-F*	GATTTTAAGATTGGCTTTGATTGA	sense	Murf2 pre PCR	97
Murf2P-R*	AATATAAAATCTAGATCAAACCATCACA	antisense		
Murf2E-F*	GATTTTAATGTTTGGTTGTTTTAATTTAG	sense	Murf2 edit PCR	126
Murf2E-R*	AATATAAAATCTAGATCAAACCATCACA	antisense		
CR4P-F*	GGGTTTAGAAGAGGACGAAATTGA	sense	CR4 prce PCR	67
CR4P-R*	CCACACTTTCTCCCCAACTAAAA	antisense		
CR4E-F*	GTGTTTGTGTTTTATGTACAGTTTATGG	sense	CR4 edit PCR	84
CR4E-R*	AACATACCCACACAAACAAACAACA	antisense		
ND3P-F*	GAATGGGAGATGGGTTTTGG	sense	ND3 pre PCR	72
ND3P-R*	AACAAATCTCTTTACCCCCTTCAG	antisense		
ND3E-F*	TGTTTTCGTTGTTGTTTGTGGTT	sense	ND3 edit PCR	72
ND3E-R*	CAATGTATAAAACACCAAACGTGAATT	antisense		
RPS12P-F*	CGACGGAGAGCTTCTTTTGAATA	sense	RPS12 pre PCR	68
RPS12P-R*	CCCCCCACCCAAATCTTT	antisense		
RPS12E-F*	CGTATGTGATTTTTGTATGGTTGTTG	sense	RPS12 edit PCR	98
RPS12E-R*	ACACGTCGGTTACCGGAACT	antisense		
ND4-F*	CAATCTGACCATTCCATGTGTGA	sense	ND4 PCR	89
ND4-R*	TTTCAGCACAATACTTGCTAATAAAACA	antisense		
REH1-F	GTAACGCGGTCCCAGTGAATCCT	sense	REH1 PCR	75
REH1-R	GTCCCTTCGACAGCCAATCAGGT	antisense		
CO I-F	CCCGATATGGTATTTCCTCGTATAAA	sense	CO I PCR	103
CO I-R	CCCCCATACCCTCTTCAGTCA	antisense		
18S rRNA-F*	CGGAATGGCACCACAAGAC	sense	18S rRNA PCR	64
12S rRNA-R*	TGGTAAAGTTCCCCGTGTTGA	antisense		
A6 PE-P1	TGATCTTATTCTATAACTCCAATAACAAACC	antisense	A6 partial edited PCR	
A6 PE-P2	GTTAGGGGGAGGAGAGAAGTTATTA	sense	A6 1st block PCR (with A6 PE P1)	74
A6 PE-P3	TAGAAGAAAGAGCAGTTGATAATGGAT	sense	A6 1st + 2nd blocks PCR (with A6 PE P1)	129
A6 PE-P4	GAATTGCCTTTGCCATATTACAGTTA	sense	A6 1st + 2nd + 3rd blocks PCR (with A6 PE P1)	166
Cyb PE-P1	AACAACCTGACATTAAAAGACAACAC	antisense	Cyb 1st block PCR	65
Cyb PE-P2	AAGCGGAGATTATTATTTTTTTTAT	sense		
Primer Extension				
A6-prob	TAACTCCAATAACAAACCAA	antisense	Oligo probe A6 1st block	
In vitro transcription template for Lt A6 partial edited mRNA				
A6PE1	CGAACT TAATACGACTCACTATAGGGAGA GCGAATAGGAAGGGATCCAGAAAGGAAATT AGTAAGACCGAGTTAATGTT	sense	template for Lt A6 partial edited gene	
A6PE2	AATAACACGAATCATAAACAAATAAAC ATACATAAACCAACAAATAAATAAACATC AAAAATACAAAACATTAACTCGGTCTTACTAATTTCC	antisense		
A6PE-F	CGAACTTAATACGACTCAC	sense	Lt A6 partial edited gene PCRpGEM-LtA6PE	
A6PE-R	AATAACACGAATCATAAACAAATAAACATA	antisense		

*Primers were derived from ref. 1.

1. Carnes J, Trotter JR, Ernst NL, Steinberg A, Stuart K (2005) An essential RNase III insertion editing endonuclease in *Trypanosoma brucei*. *Proc Natl Acad Sci USA* 102:16614–16619.

Table S2. RNA oligonucleotides

Oligonucleotide name	Sequence
Lt A6 partial edited mRNA	GGGCGAATTCGCGAAUAGGAAGGGAUCCAG AAAGGAAAUUAGUAAGACCGAGUUAAUG UUUUGUAUUUUUGAUGUUUAUUUAUUU GUUGGUUUAUGUAUGUUUAUUUGUUUAUGAUUCGUGUUAUU
Lt gA6 II	AUAAACCAACAAAUAAAUAAAUGUCAGA GAUACAAGAUAUUAAUUUUUUU
RNA-I	AAGAAGCAUAAUGUUCUUUUUAUAUUUAUCGUGUAGU
RNA-II	ACUACACGAUAAAUAUAAAAAG
RNA-III	AACAUUAUGCUUCUU
RNA-IV	AAGAAGCAUAAUGUU

Table S3. Sequences derived from MS/MS and manual sequencing of peptides recovered via trypsin in-gel digestion of the protein bands in Fig. 3*C*

Band I TEV-protease (70 kDa)	Band I LmjF32.0400 (70 kDa)	Band II Lm REH1-SBP	Band III C-term of Lm REH1-SBP
FPQVAATGDGPDIIFWAHDR	GFNDVQGGYVGGFNR	LGSLVEDGTIDDNKDKLIIFVER	EFMPR
TWEEIPALDKELK	AKPTNSQSAPSALVLSPTR	ELTQLAESYQHR	KRDDDLPSTLDWSSR
EFLENYLLTDEGLEAVNK	FLVLDEADR	SENSSGFGR	DDDLPSTLDWSSR
SYEEELAKDPR	GLDIPNVAVVVQYDLPSNIDDYVHR	KRDDDLPSTLDWSSR	GGHVVEGLAGELEQLR
ESLFKGPR	GTAISFFNDKNR	GGHVVEGLAGELEQLR	ARLEHHPQGQR
NTTTLQQHLIDGR	NIVDDLIPLLR		LGLLVPR
FREPQREER			